Proceedings of the ASME 2014 International Design Engineering Technical Conferences & Computers and Information in Engineering Conference
IDETC/CIE 2014
August 17-20, 2014, Buffalo, New York, USA

DETC2014-34409

IDENTIFICATION OF NONLINEAR BEHAVIOR IN A COMPOSITE STRUCTURE WITH CORE-CRUSHING DAMAGE

Janette J. Meyer*
Douglas E. Adams
Labratory for Systems Integrity and Reliability
Department of Civil & Environmental Engineering
Vanderbilt University
Nashville, Tennessee 37235
Email: janette.j.meyer@vanderbilt.edu

Eric R. Dittman

School of Mechanical Engineering
Purdue University
West Lafayette, Indiana 47907

ABSTRACT

Many damage detection methods that are applied to composite structures rely on nonlinear features in the dynamic response of the structure to identify the presence of defects. Presently, there is not a complete understanding of the physical mechanisms that cause the nonlinear behavior of a damaged composite structure. Correlating specific types of damage mechanisms to the resulting nonlinear response characteristics they cause would allow the detection methods to classify the type of damage that is present in the structure. In this work, a drop tower was used to impact an aluminum honeycomb sandwich panel in order to induce core-crushing. The response of the damaged panel to sinusoidal excitations of various amplitudes at resonant, super-, and sub-harmonic frequencies was then measured. The amplitudes of these measured responses and the corresponding restoring force curves were then compared to a predictive model to identify the type of theoretical nonlinearity (i.e. quadratic or cubic stiffness, quadratic or cubic damping, etc.) that was present. The predictive model is based on a nonlinear, single degree-of-freedom system. Nonlinear features in the response of the system were identified for different types of stiffness and damping nonlinearities. The experimentally measured response was analyzed to see which of these features were present. Based on this analysis, the response of the panel of damage due to core-crushing indicated a quadratic spring-type stiffness.

INTRODUCTION

Composite materials are being used more frequently in engineering applications due to their high strength-to-weight ratios, corrosion resistance, and other favorable material properties. Unlike standard metals, composite materials can experience complex damage mechanisms, including facesheet disbonds, delamination between bonded layers, and core-crushing, which are difficult to detect using traditional damage detection methods. Much research has been conducted to develop methods which identify the presence of damage in composite materials, and many of these methods are based on nonlinear techniques [1–3]. These methods are typically based on the assumption that non-damaged (healthy) materials exhibit nearly linear response characteristics while the response of damaged materials contain nonlinear features that can be quantified to indicate the presence of damage. In many cases, these methods are successful even when the physics of the damage mechanism are not well understood. Furthermore, although these methods can detect the presence of damage, most are unable to identify the type of damage that is present without a prioi knowledge. A better understanding of the correlation between the type of damage present in a composite material and the nonlinear features present in its response spectrum could allow damage detection methods to not only identify the presence of damage, but also to classify its type.

Previously [4, 5], a method was presented for studying the nonlinear effects of different damage mechanisms using a single

*Address all correspondence to this author.

degree-of-freedom model. In that work, the equation of motion for a single degree-of-freedom system with second- and third-order stiffness and damping nonlinearities was solved for the system response due to an excitation at the natural frequency and sub-resonant frequencies. Trends in the force-deflection curve were noted for each type of nonlinearity and at each frequency of excitation. Corresponding experimental data was acquired from an aluminum honeycomb panel with disbond damage. The response characteristics in the experimental data were compared to the results from the analytical model to determine which type of theoretical nonlinearity (i.e. quadratic or cubic stiffness, quadratic or cubic damping, etc.) best described the disbond damage. In this work, a similar approach will be taken to identify the nonlinear behavior in a honeycomb sandwich panel with core-crushing damage. In the following sections, the analytical analysis presented in [5] will be summarized. Then, the setup and procedure for acquiring experiential data from aluminum honeycomb composite panels with core-crushing damage will be described. Finally, a comparison between the results from the analytical model and the experimental results will be made in order to identify the type of theoretical nonlinearity that best describes the core-crush damage.

Analytical Model and Nonlinear Analysis

In [5], an approach similar to that used in [6] was applied to the single degree-of-freedom system with second- and third-order nonlinearities described by

$$\ddot{u} + 2\mu\dot{u} + \omega_o^2 u + f(u,\dot{u}) = F cos(\Omega t)$$

$$\text{where } f(u,\dot{u}) = \begin{cases} \kappa u^3, & \text{for a cubic stiffness} \\ \kappa u^2, & \text{for a pure quadratic stiffness} \\ \kappa u|u|, & \text{for a rectified quadratic stiffness} \\ \kappa \dot{u}^3, & \text{for cubic damping} \\ \kappa \dot{u}^2, & \text{for pure quadratic damping} \\ \kappa \dot{u}|\dot{u}|, & \text{for rectified quadratic damping} \end{cases} \tag{1}$$

where u is the displacement of the system, μ is the linear damping coefficient, ω_o is the natural frequency of the system, and κ is a coefficient of nonlinearity. Using the method of multiple time scales or the method of averaging [7], the response, u in Equation 1 was determined for each case of nonlinearity for two different frequencies of excitation. For the cases of quadratic nonlinearities, the response at excitation frequencies of $\Omega = \omega_o$ and $\frac{1}{2}\omega_o$ were estimated. For cubic nonlinearities, the response at excitation frequencies of $\Omega = \omega_o$ and $\frac{1}{3}\omega_o$ were estimated. For each excitation frequency, the solution was obtained for a range of forcing amplitudes (F) so that force-deflection curves could be plotted. For quadratic nonlinearities, trends in the force-deflection curve were determined using the response at ω_o and the response at $2\omega_o$. For cubic nonlinearities, trends in the force-deflection curve were determined using the response at ω_o and the response at $3\omega_o$. Table 1 summarizes these trends.

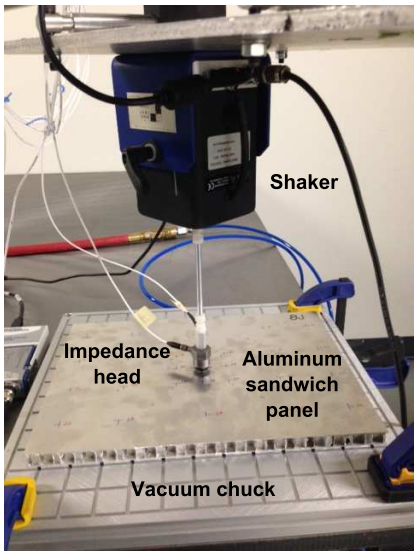

FIGURE 1: Experimental setup.

Experimental Setup and Procedure

Composite aluminum panels (22.5 x 29.5 x 1 cm) each comprised of an aluminum honeycomb core sandwiched between two aluminum facesheets were used for the experimental analysis. The experimental setup and fixture was devised in order to exploit the single degree-of-freedom analysis described above. The setup is shown in Figure 1. A vacuum chuck was chosen to secure the bottom facesheet of the panel for two reasons. First, the vacuum chuck eliminated the need for any external clamping which could introduce unwanted nonlinearity into the system. Second, by securing the bottom facesheet, the sandwich panel can be thought of as a single degree-of-freedom system in which the top face sheet acts as the mass and the honeycomb core acts as the stiffness and damping mechanisms. This assumption that the panel will behave as a single degree-of-freedom system allows the results from the single degree-of-freedom analytical model to be relevant.

Core-crush damage was imposed on the panels using impacts from an Instron Dynatup drop tower with 5 cm tup installed. Three levels of damage were introduced by making impacts three different energy levels: 2, 4, and 8 J. The energy calculations were done internally as a part of the drop tower software. Figure 2 shows the anticipated levels of core-crush on a

TABLE 1: Summary of nonlinear trends observed in the analytical data.

Nonlinearity Type	Excitation with amplitude F at ω_o		Excitation with amplitude F at $\frac{1}{2}\omega_o$ or $\frac{1}{3}\omega_o$	
	Response at ω_o with respect to F	Response at $2\omega_o$ or $3\omega_o$ with respect to F	Response at ω_o with respect to F	Response at $2\omega_o$ or $3\omega_o$ with respect to F
Quadratic Stiffness	1-to-1	Quadratic	Quadratic	Quartic
Quadratic Damping	1-to-1	To the 1.2 power	Quadratic	Zero
Cubic Stiffness	1-to-1 on backbone curve	Undetermined	Cubic on the backbone curve	Undetermined
Cubic Damping	To the 0.8 power	Undetermined	To the 2.75 power	Undetermined

(a) 2 J (b) 4 J (c) 8 J

FIGURE 2: Core-crushing damage created by impacts with the indicated energy level.

surrogate panel. Visible damage was apparent on the facesheet that was impacted, especially for the 8 J impact. When mounting the damaged panels into the experimental fixture, the facesheet that was impacted was placed face down.

To measure the force and response of each panel, a PCB 288D01 impedance head, which measures both force and acceleration, was mounted to the center of the panel. A TMS Mini-SmartShaker with nylon stinger and a standard function generator was used to excite the panel. A National Instruments 9234 four-channel data acquisition card was used with MATLAB software to acquire the sensor time histories, and data analysis was performed using MATLAB.

Impact and sine-sweep tests were conducted to identify the primary natural frequency, ω_o, to be used for each panel. The response of each panel to a harmonic excitation at ω_o, $\frac{1}{2}\omega_o$, and $\frac{1}{3}\omega_o$ was then measured. Excitation at these three frequencies were repeated at multiple force amplitudes. Finally, slow, narrow-band sine sweeps in the vicinity of each excitation frequency were conducted in order to identify potential backbone trends. The frequencies and force levels used for each panel are shown in Table 2. For each amplitude and frequency of input

TABLE 2

Damage		Excitation Frequency (Hz)	Force Range (N)
2 J	ω_o	693.4	1.1-20.3
	$\frac{1}{2}\omega_o$	346.7	0.1-4.4
	$\frac{1}{3}\omega_o$	231.1	0.1-5.2
4 J	ω_o	589.6	1.0-19.3
	$\frac{1}{2}\omega_o$	294.8	0.1-7.3
	$\frac{1}{3}\omega_o$	196.5	0.1-5.7
8 J	ω_o	587.8	1.2-18.3
	$\frac{1}{2}\omega_o$	293.9	0.1-4.7
	$\frac{1}{3}\omega_o$	195.9	0.1-5.7

excitation, response amplitudes were recorded at the forcing frequency (ω_o, $\frac{1}{2}\omega_o$, or $\frac{1}{3}\omega_o$), at $2\omega_o$, and at $3\omega_o$. When exciting at $\frac{1}{2}\omega_o$ and $\frac{1}{3}\omega_o$, the amplitude of response at ω_o was also recorded. These amplitudes were then plotted as a function of forcing amplitude.

Results

For each force level and frequency listed in Table 2, the response spectrum of the acceleration response was calculated. Figure 3 shows the spectrum for the 8 J damage case panel when forced at 587.8 Hz. In addition to the response at the excitation frequency, clear peaks at twice- and three-times the excitation frequency are evident. As described in the previous section,

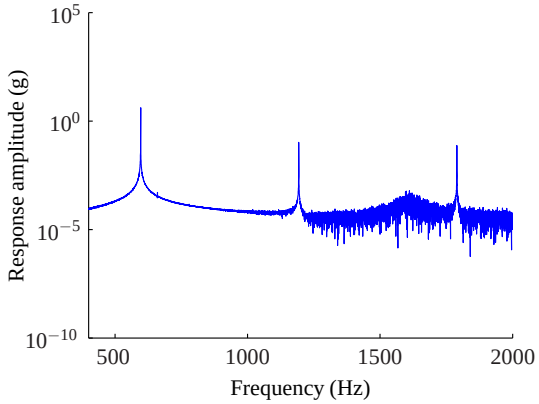

FIGURE 3: Response spectrum of the aluminum panel (8 J damage case) to an excitation force of 10 N at 587.8 Hz.

the amplitudes of response at each frequency of interest were recorded for each test. Results from the slow sine sweeps performed in the vicinity each excitation frequency of interest did not show any backbone trends, which would have been one indicator of cubic nonlinearities. Therefore, those results are not included here.

Figure 4 shows the force-response curves and the normalized response-force curves for each damage case for responses measured at the frequency of excitation. The force-response curves show that there is a linear relationship between the amplitude of the applied force and the amplitude of response. As expected, as the damage level increases, the stiffness, indicated by the slope of the line, decreases. The expected one-to-one relationship between the amplitude of the force and the amplitude of response is shown in the normalized response-force curves.

Figure 5 shows that relationship between the forcing at ω_o and the amplitude of response at $2\omega_o$ and $3\omega_o$. The nearly quadratic trend present for the response at $2\omega_o$ suggests the presence of a quadratic stiffness nonlinearity, according to Table 1. The trend in the response at $3\omega_o$ is less conclusive. A cubic trend would have been expected if a cubic stiffness-type nonlinearity was present, but this trend is not evident. The data is more closely approximated by a quadratic curve, indicated by the black line in the plot.

To further explore the possibility of the presence of a quadratic nonlinearity, trends in the response amplitudes at ω_o and $2\omega_o$ to a force at $\frac{1}{2}\omega_o$ were considered. Figure 6 shows the corresponding plots. The response amplitudes at ω_o appear to grow quadratically with the forcing amplitude, further supporting the presence of a quadratic stiffness-type nonlinearity. (See Table 1.) In theory, the response at $2\omega_o$ should grow quartically in the presence of a quadratic stiffness. Figure 6 b indicates that the response at $2\omega_o$ is growing at a lesser rate, especially as damage increases. This decrease in growth rate may indicate an increasing effect of damping as the amplitude of response increases.

Finally, the response amplitudes at ω_o and $3\omega_o$ to a force at $\frac{1}{3}\omega_o$ were considered. Up to this point in the analysis, no trends have been observed that support the presence of a cubic nonlinearity based on the indicators listed in Table 1. Figure 7 a provides further evidence that the data does not follow the theoretical trend for a cubic stiffness or damping nonlinearity.

Discussion

Based on the above analysis, there is strong evidence to support the presence of a quadratic stiffness-type nonlinearity in the damaged panels. The practical use of this conclusion would be that a lumped-parameter model of the composite panel should include quadratic spring stiffnesses. Physically, this conclusion implies that the panel has amplitude-dependent stiffness properties. In a healthy panel, it is expected that the stiffness of the honeycomb core is nearly linear. However, when the core has been crushed, some or all of the cell walls of the core have been buckled. This buckling effect means that the ability of the core to resist motion is dependent on the amplitude of excitation, producing the nonlinear effects discussed above.

The nature of the cubic nonlinearity is more difficult to assess. Based on the single degree-of-freedom metrics presented in Table 1, there is no indication that a cubic nonlinearity is present. However, a distinct response was observed in the panels at three-times the excitation frequency, which is indicative of a cubic nonlinearity. There are several possible explanations for this contradiction. First, the single degree-of-freedom model may not be capable of capturing the dynamics that are causing the cubic response in the panel. Although the experimental setup was devised to approximate a single degree-of-freedom system, the panel is a continuous system capable of multi-dimensional motions. Second, it is likely that when two types of (theoretical) nonlinearities are present in a system, complex interactions between the response caused by each individual nonlinearity take place. In other words, the superposition of the effects of two different nonlinearities may not accurately predict the total effect that both nonlinearities have on the system response. One possible means for exploring this idea is to extend the results presented in Table 1 to include the trends observed in the presence of combinations of different types of nonlinearities.

Conclusions

Previously, a nonlinear single degree-of-freedom model was developed and used to correlate nonlinear features in the response of the system with the type of nonlinearity present. In this work, damaged composite panels were tested in order to identify the types of theoretical nonlinearities present, as predicted by the single degree-of-freedom model. Three composite aluminum honeycomb sandwich panels with varying levels of core-crushing

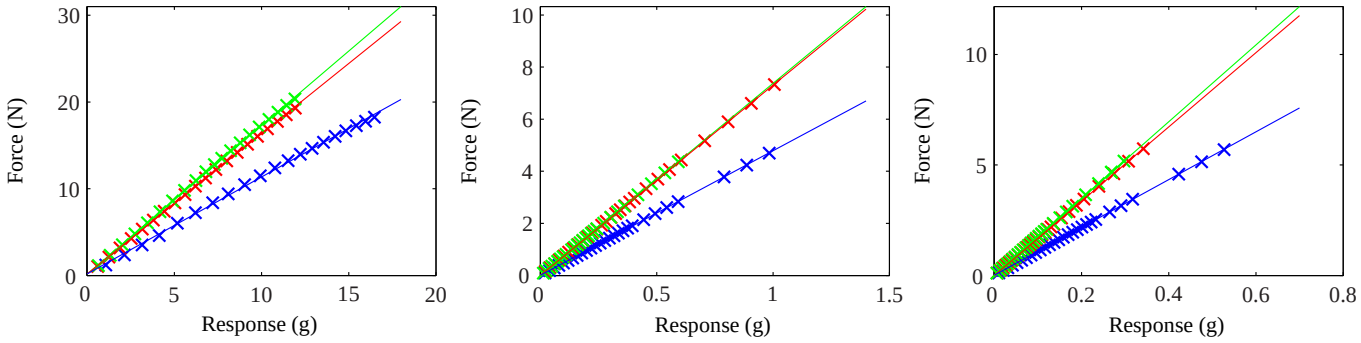

(a) Magnitude of response at ω_o versus magnitude of force at ω_o.

(b) Magnitude of response at $\frac{1}{2}\omega_o$ versus magnitude of force at $\frac{1}{2}\omega_o$.

(c) Magnitude of esponse at $\frac{1}{3}\omega_o$ versus magnitude of force at $\frac{1}{3}\omega_o$.

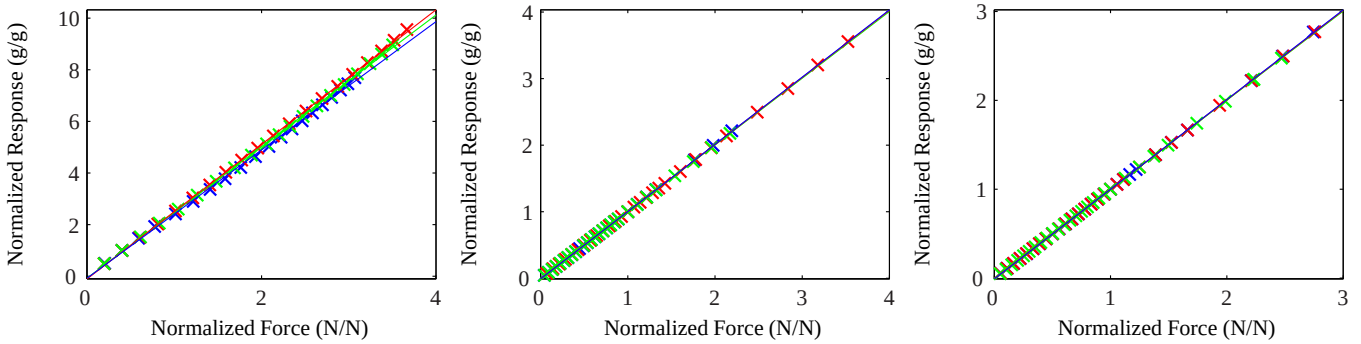

(d) Normalized magnitude of response at ω_o versus normalized magnitude of force at ω_o.

(e) Normalized magnitude of response at $\frac{1}{2}\omega_o$ versus normalized magnitude of force at $\frac{1}{2}\omega_o$.

(f) Normalized magnitude of response at $\frac{1}{3}\omega_o$ versus normalized magnitude of force at $\frac{1}{3}\omega_o$.

FIGURE 4: Force-response curves (a-c) and normalized response-force curves (d-f) for responses measured at the frequency of excitation for the 2 J (×), 4 J (×), and 8 J (×) damage cases.

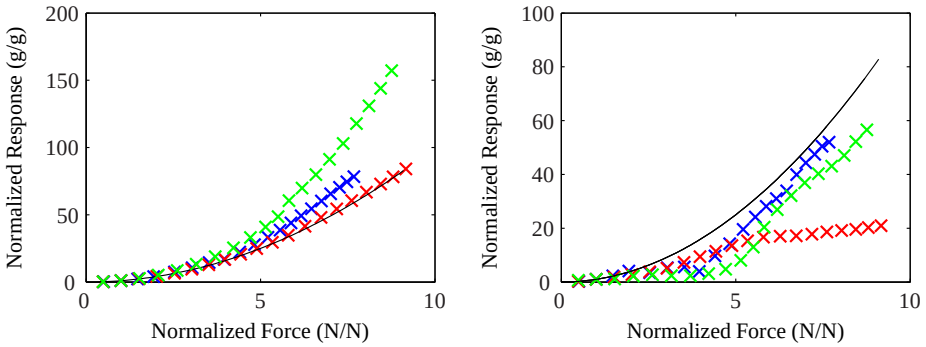

(a) Normalized magnitude of response at $2\omega_o$ versus normalized magnitude of force at ω_o.

(b) Normalized magnitude of response at $3\omega_o$ versus normalized magnitude of force at ω_o.

FIGURE 5: Normalized response-force curves for forcing at ω_o for the 2 J (×), 4 J (×), and 8 J (×) damage cases. (—) indicates a quadratic curve.

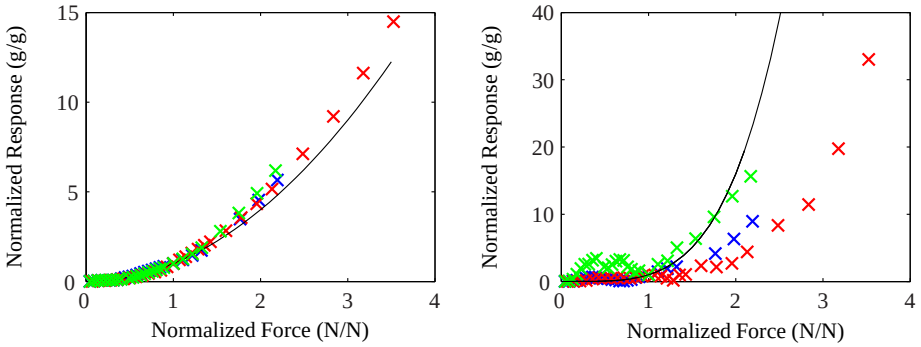

(a) Normalized magnitude of response at ω_o versus normalized magnitude of force at $\frac{1}{2}\omega_o$.

(b) Normalized magnitude of response at $2\omega_o$ versus normalized magnitude of force at $\frac{1}{2}\omega_o$.

FIGURE 6: Normalized response-force curves for forcing at $\frac{1}{2}\omega_o$ for the 2 J (×), 4 J (×), and 8 J (×) damage cases. In (a), (—) indicates a quadratic curve. In (b), (—) indicates a quartic curve.

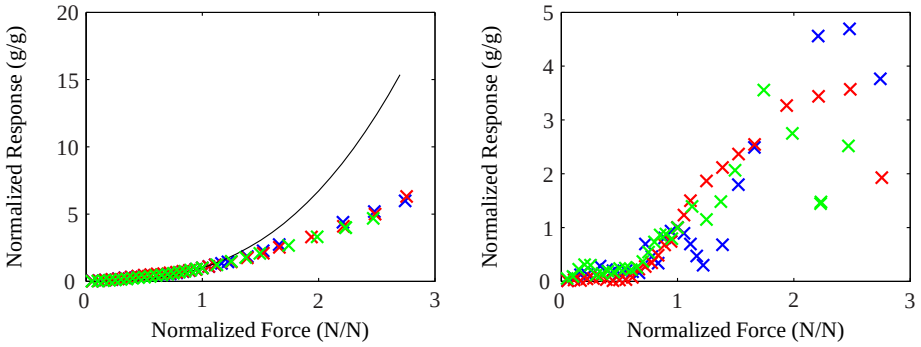

(a) Normalized magnitude of response at ω_o versus normalized magnitude of force at $\frac{1}{3}\omega_o$.

(b) Normalized magnitude of response at $3\omega_o$ versus normalized magnitude of force at $\frac{1}{3}\omega_o$.

FIGURE 7: Normalized response-force curves for forcing at $\frac{1}{3}\omega_o$ for the 2 J (×), 4 J (×), and 8 J (×) damage cases. In (a), (—) indicates a 2.75 power law curve.

damage were tested in a fixture designed to approximate a single degree-of-freedom system. The relationship between the amplitude of response of the panel and the amplitude of the applied force was considered at multiples of the excitation frequencies. A nearly quadratic relationship was observed between the response amplitudes at twice the excitation frequency and the amplitude of the force when exciting at the natural frequency and at half of the the natural frequency of the system. Although the response spectra included a strong response at three-times the excitation frequencies, the trends in the response-force curves did not match those predicted by the single degree-of-freedom model for cubic nonlinearities. The most likely explanation for this contradiction is that the effects of the presence of two types of nonlinearities are not described by superimposing the effects of each individual nonlinearity. Future work will extend the analysis of the single degree-of-freedom model to include trends observed in the presence of multiple nonlinearities.

REFERENCES

[1] Van Den Abeele, K.-A., Carmeliet, J., Ten Cate, J. A., and Johnson, P. A., 2000. "Nonlinear elastic wave spectroscopy (news) techniques to discern material damage, part ii: Single-mode nonlinear resonance acoustic spectroscopy". *Journal of Research in Nondestructive Evaluation*, ***12***(1), pp. 31–42.

[2] Farrar, C. R., Worden, K., Todd, M. D., Park, G., Nichols, J., Adams, D. E., Bement, M. T., and Farinholt, K., 2007. Nonlinear system identification for damage detection. Tech. rep., Los Alamos National Laboratory (LANL), Los Alamos, NM.

[3] Polimeno, U., Meo, M., Almond, D., and Angioni, S.,

2010. “Detecting low velocity impact damage in composite plate using nonlinear acoustic/ultrasound methods”. *Applied Composite Materials,* ***17***(5), pp. 481–488.

[4] Dittman, E., and Adams, D., 2013. “Detection and quantification of a disbonded aluminum honeycomb panel using nonlinear superhamonic frequencies”. In Proceedings of the 9th International Workshop on Structural Health Monitoring at Stanford, 2013.

[5] Dittman, E., 2013. “Identification and quantification of nonlinear behavior in a disbonded aluminum honeycomb panel using single degree-of-freedom models”. PhD thesis, Purdue University.

[6] Andreaus, U., Casini, P., and Vestroni, F., 2007. “Non-linear dynamics of a cracked cantilever beam under harmonic excitation”. *International Journal of Non-Linear Mechanics,* ***42***(3), pp. 566 – 575.

[7] Nayfeh, A., and Mook, D., 1995. *Nonlinear Oscillations*. Wiley-VCH.